Supplementary Information (SI) for Lab on a Chip.

Three-dimensional inertial focusing based impedance cytometer enabling high-accuracy characterization of electrical properties of tumor cells

Chen Ni, Mingqi Yang, Shuai Yang, Zhixian Zhu, Yao Chen, Lin Jiang, and Nan Xiang*

School of Mechanical Engineering, and Jiangsu Key Laboratory for Design and Manufacture of Micro-Nano Biomedical Instruments, Southeast University, Nanjing, 211189, China.

*E-mails: nan.xiang@seu.edu.cn.

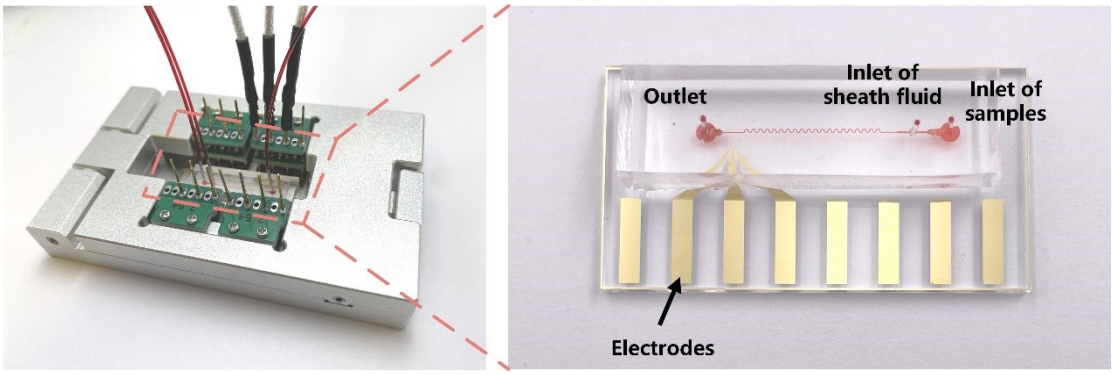

Figure S1. Photographs of the impedance cytometer and a close-up of the microchannel. The microchannel was filled with red dye for visualization.

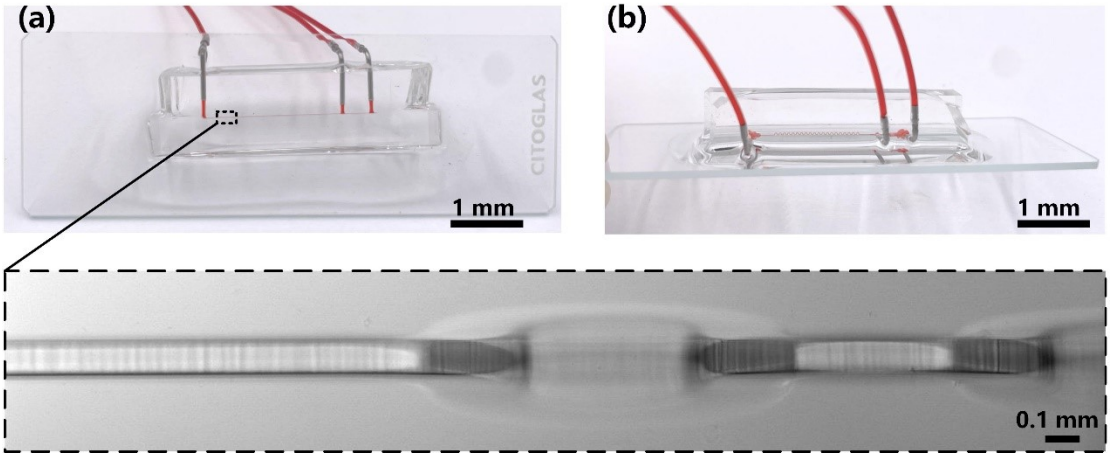

Figure S2. Photographs of the chip used to observe the particle trajectories in channel height direction, and side view of the channel observed using a 10x objective. (a, b) Photographs of the chip viewed from the bottom (a) and side (b), respectively. The microchannel was filled with red dye for visualization.

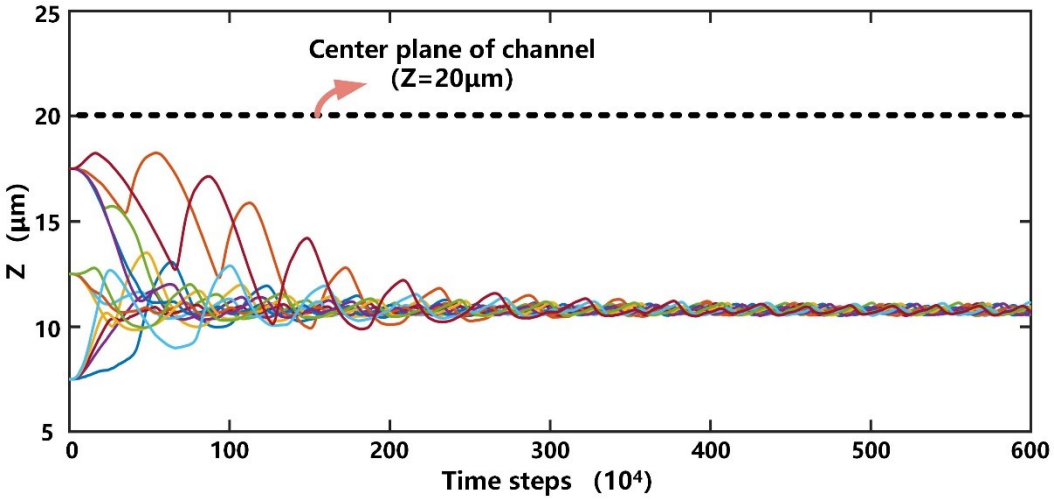

Figure S3. Simulation results of vertical trajectories of particles released at different initial positions.

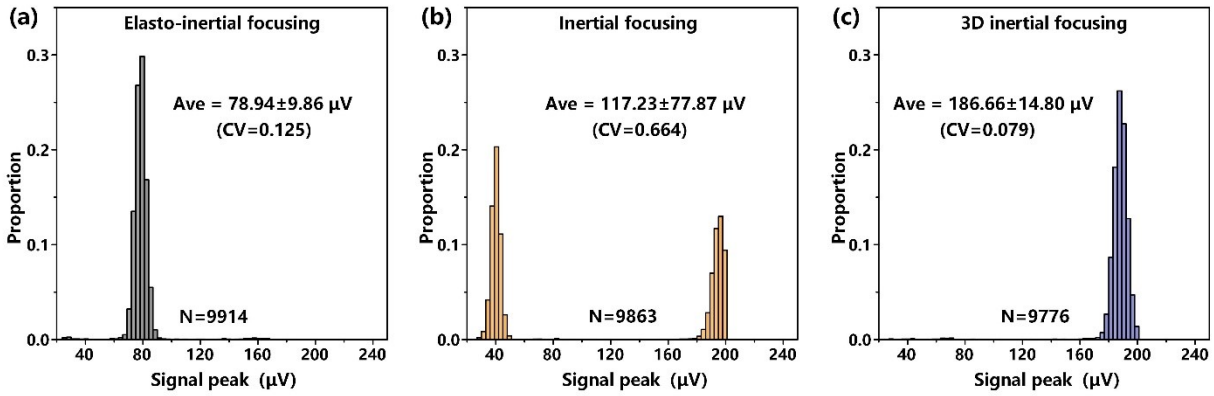

Figure S4. Histograms for peak amplitude distribution of the 10 μm particle impedance signals under the three focusing methods and the corresponding CV.

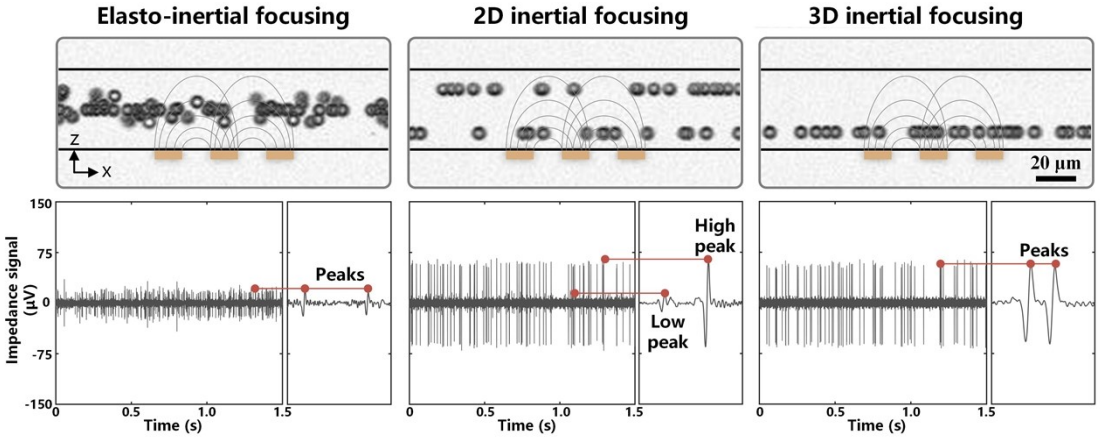

Figure S5. Distributions of 7 μm particles in the vertical direction and impedance signals in the detection area using the three focusing methods. The AC frequency used in this experiment was 0.5 MHz.

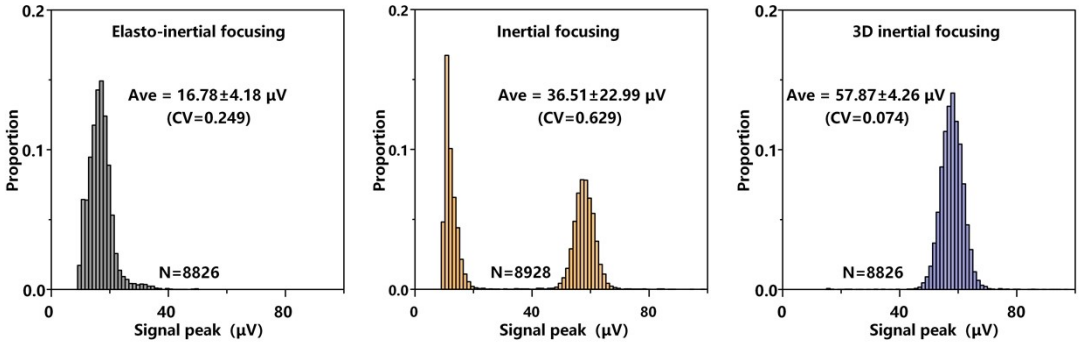

Figure S6. Histograms for peak amplitude distribution of the 7 μm particle impedance signals under the three focusing methods and the corresponding CV.

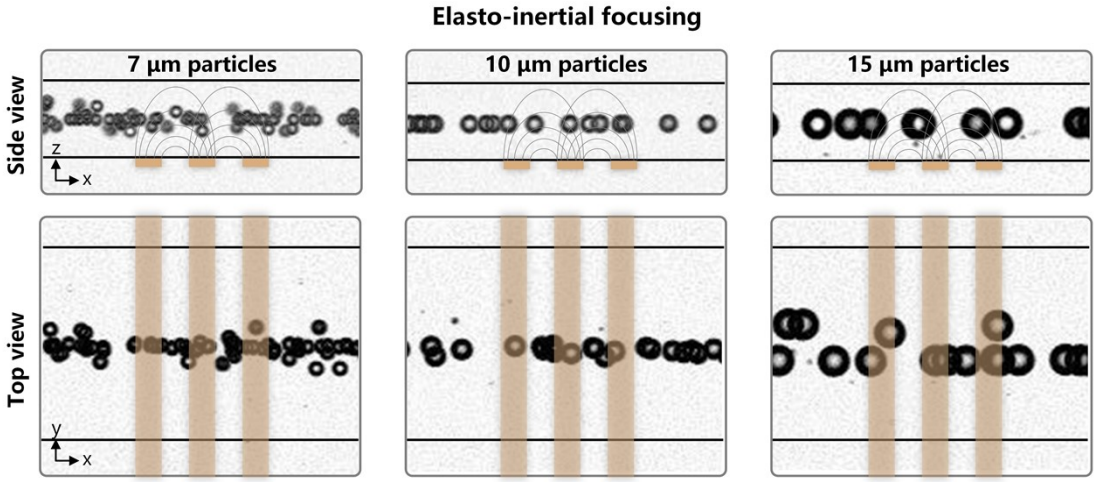

Figure S7. Distributions of 7 μm, 10 μm, and 15 μm particles at the microchannel outlet under top and side views. The flow rate is 200 μl/min.

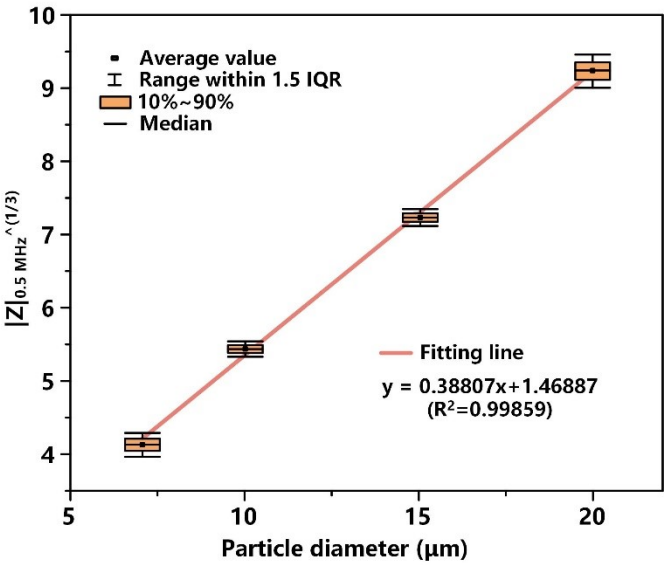

Figure S8. Distribution of the cube root of peak amplitude of particles with different particle sizes (7μm, 10μm, 15μm, 20μm) and corresponding fitting line. (N=1000 for each particle). The AC frequency used in experiment was 0.5 MHz.

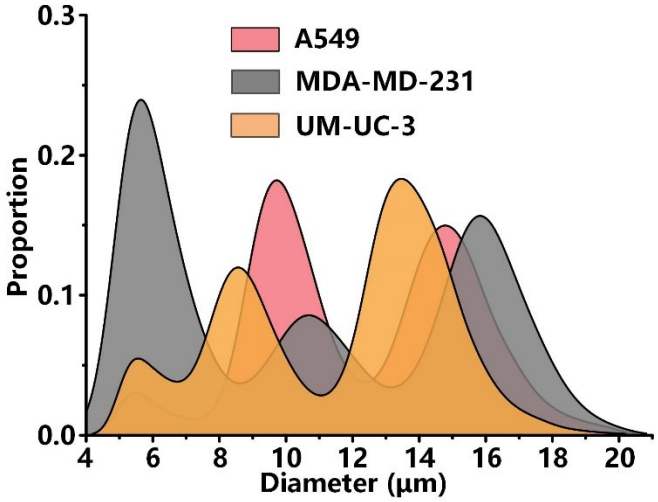

Figure S9. Diameter distributions of A549, MDA-MB-231, and UM-UC-3 cells under traditional 2D inertial focusing.

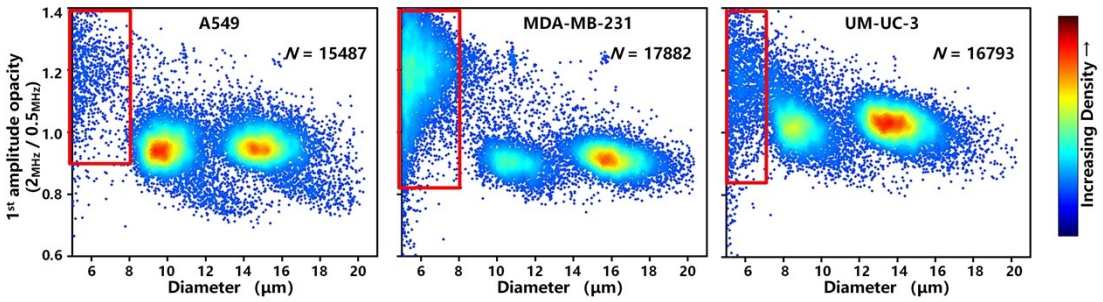

Figure S10. Scatter plots of 1st amplitude opacity versus cell diameter for A549, MDA-MB-231, and UM-UC-3 cells under traditional 2D inertial focusing.

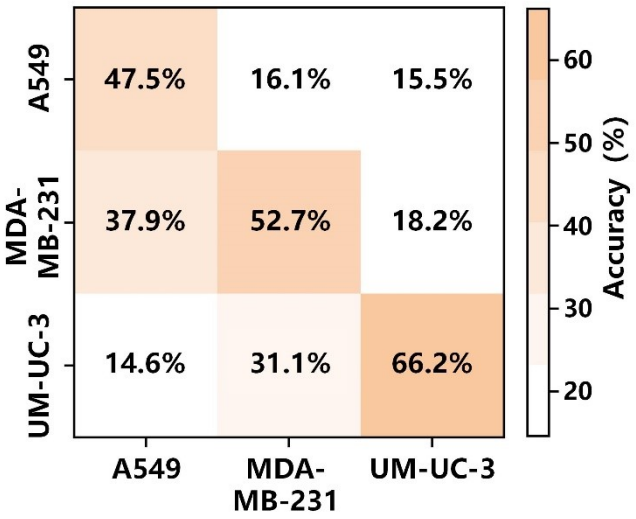

Figure S11. Confusion matrix of machine learning results using parameters of cell diameter, 1st amplitude opacity, 1st phase opacity, 2nd amplitude opacity, and 2nd phase opacity. The focusing method is traditional 2D inertial focusing.